Appendix 12 – Bundaberg Case Study

This study site comprised a 24.7 ha area within the Hubert family farm in the Gooburrum district of the Bundaberg canegrowing region. The site is dominated by deep acidic red clay loams of the Otoo and Watalgan series as described in a canegrowing context by Schroeder et al. 2007[1] (Figure 12.1). These are Dermosols in the terminology of the Australian soil classification. Average annual rainfall at the site is 1143 mm.

As at our other case study sites, we undertook high resolution soil survey using EM38 (Figure 12.2) and gamma radiometrics (Figure 12.4); in the case of the EM38 survey, we were also able to demonstrate through repeat surveys at this site in the presence and absence of trash, that trash does not present an impediment to the use of the EM38 sensor (Appendix 24). This was in spite of the fact that both the actual EC_a values and their range of variation was low (Figure 12.2), indicating that variation in the key soil properties which drive soil conductivity is limited at this site. It this therefore notable that overlay of the EM38-derived map (high resolution) with the 1:50,000 regional reconnaissance soil survey underpinning the management recommendations contained Schroeder et al. (2007) suggests a surprisingly accurate alignment of the boundary between the Otoo and Watalgan soil series (Figure 12.3), the main difference between these being in terms of their clay content; Watalgan contains less clay.

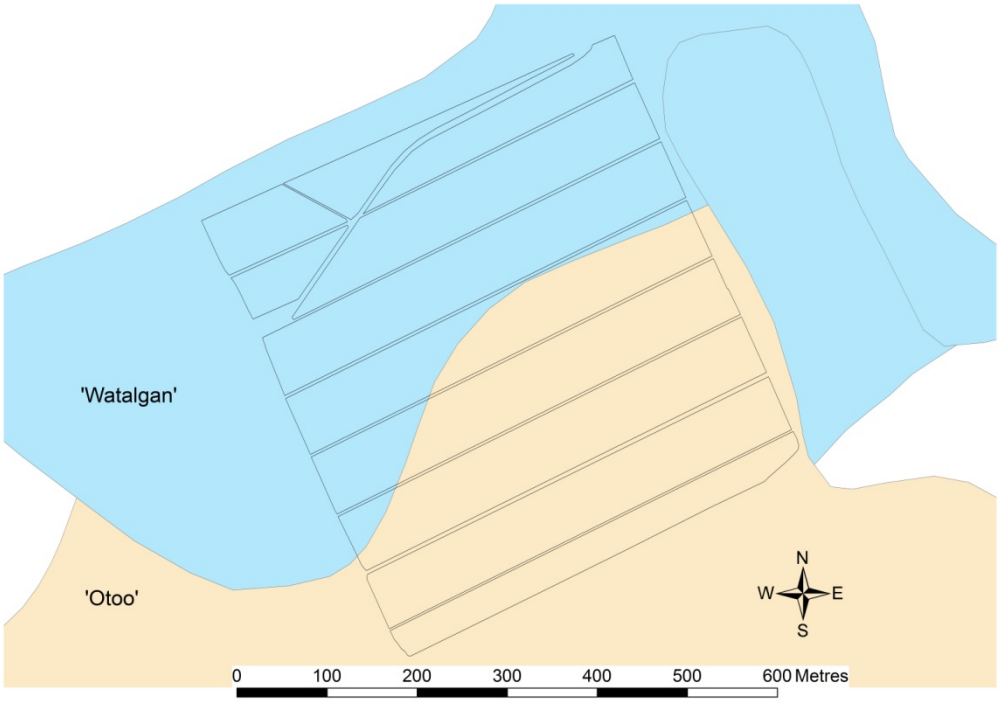

Figure 12.1 1:50,000 soil survey data of our Bundaberg study site. Data of QDNR – Land Resource Bulletin DNRQ980142.

[1]Schroeder, B., Panitz, J., Wood, A., Moody, P., Salter, B., 2007. Soil-Specific Nutrient Management Guidelines for Sugarcane Production in the Bundaberg District. Technical Publication TE07004. BSES Limited, Indooroopilly, Queensland, Australia.

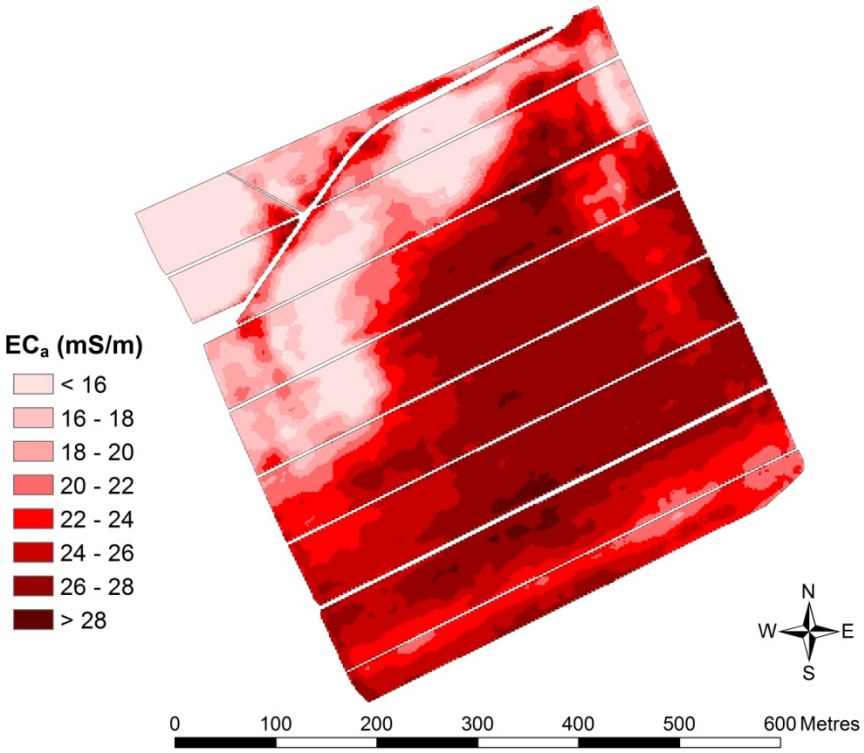

Figure 12.2 Variation in bulk electrical soil conductivity (ECa) across the Bundaberg study site as assessed using EM38.

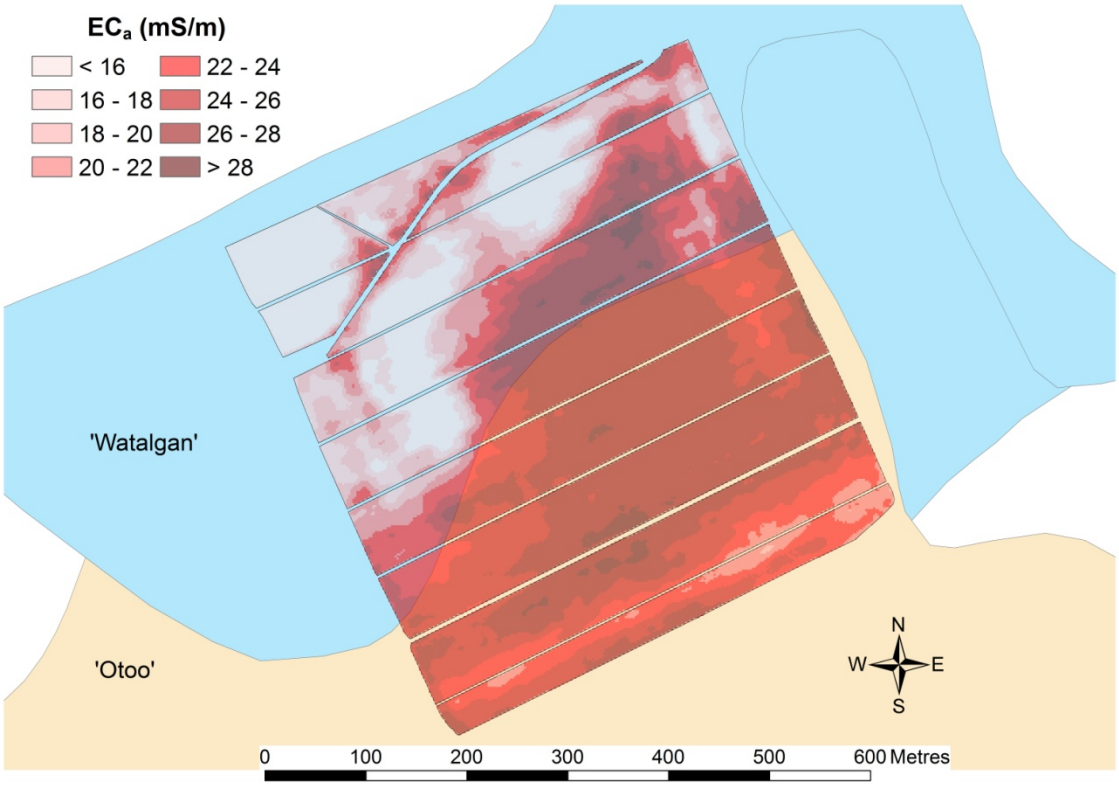

Figure 12.3 Alignment between the high resolution electromagnetic soil survey and a 1:50,000 regional reconnaissance soil map.

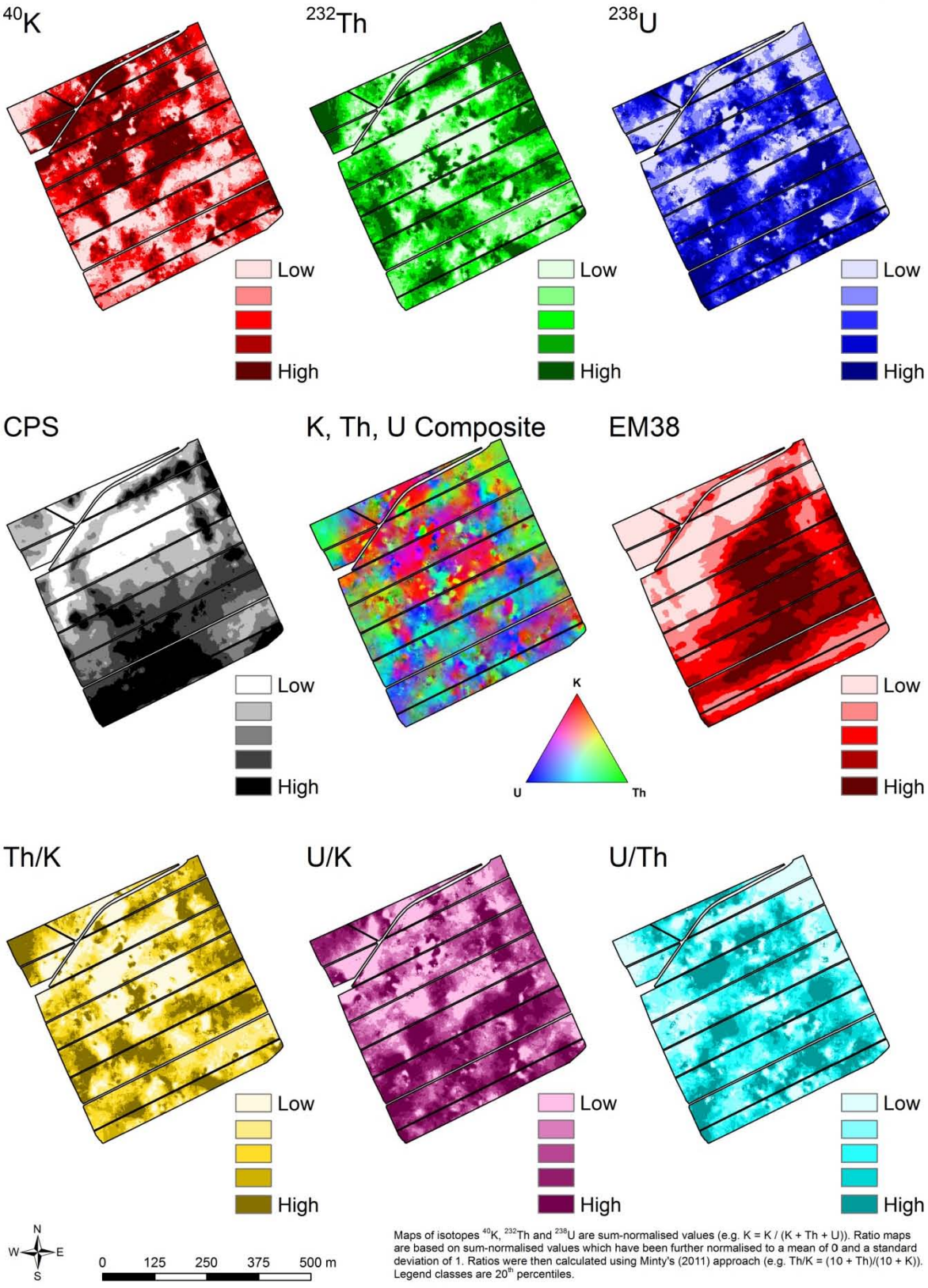

Figure 12.4 Maps derived from proximal gamma radiometric soil sensing of the Bundaberg study site. Also shown for comparison is the EM38 soil map (Figure 12.2).

There was little apparent alignment between the EM38 soil map (Figure 12.2) and the maps derived from gamma radiometrics other than with respect to the total count (CPS; Figure 12.4) which was found to be well correlated with clay content in spite of these soils having relatively low radiometric activity. Given the similarity between the Otoo and Watalgan soils (Schroeder et al. 2007), this makes the alignment between the soil surveys at different scales somewhat surprising and, in spite of the low radiometric activity of these soils, points to the potential utility of gamma radiometrics as a high resolution soil survey tool for precision agriculture (PA).

Clustering of the EM38 soil map (Figure 12.2) with a pre-project (2008) SPOT image of NDVI for the site using *k*-means (Figure 12.5) suggested that the site may be a strong candidate for PA, given the apparent close alignment between variation in crop biomass and soil variation. During the project, and in collaboration with Andrew Robson (then QDPI; SRDC project DPI021), satellite imagery was also acquired in April 2011 and 2012 from the Ikonos platform and again using SPOT in 2013 (Figure 12.6), whilst in 2011, we also acquired data on 3 occasions using the airborne 'Raptor' sensor (David Lamb, UNE), also in collaboration with SRDC project DPI021 (Figure 12.7). The patterns of variation in these images was seen to be consistent suggesting a broad stability in the patterns of variation in crop performance, both over a 6 year period (Figure 12.6) and also within season (Figure 12.7). Thus, when the annual satellite images were analysed using *k*-means clustering (Figure 12.8), the patterns of variation in crop biomass (i.e. NDVI) were seen to be constant when both 2 and 3 cluster solutions were derived. In light of this result, and since imagery is conventionally displayed using a 5-class quantile categorisation (i.e. 20% of the data in each class), we also derived a 5-cluster solution. Whilst this exhibited some minor temporal variation in the rank order of the clusters, the overall cluster pattern was easily recognisable

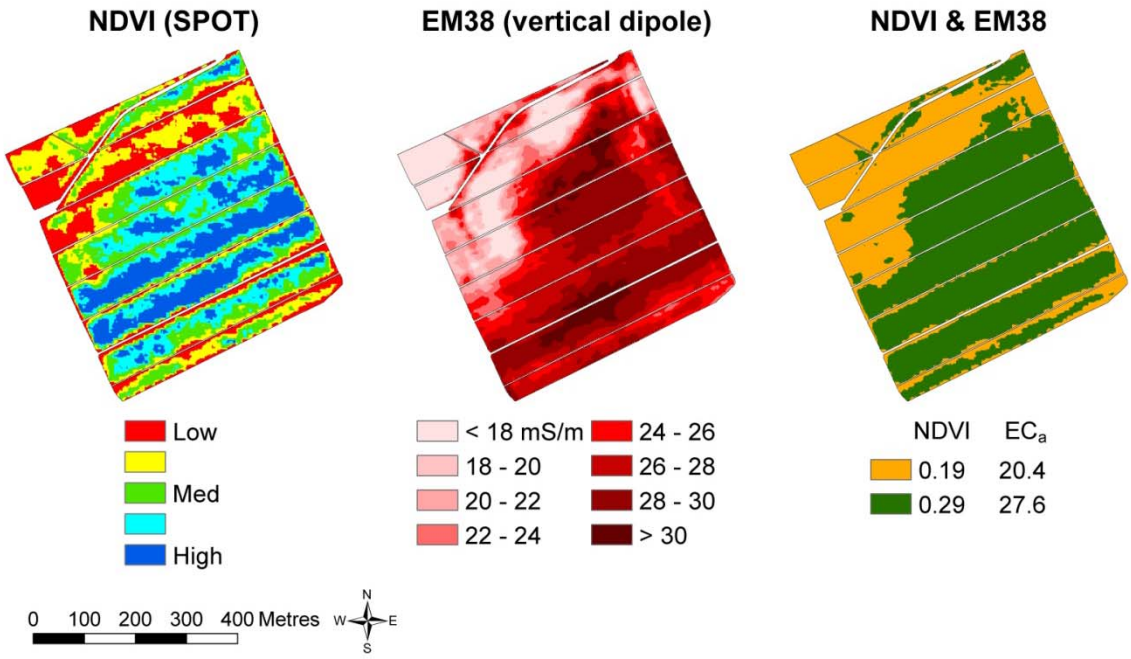

Figure 12.5 Cluster analysis of NDVI, as measured by satellite remote sensing (SPOT; March 2008), with the EM38 soil map (Figure 13.2) suggesting close alignment of soil and crop variation.

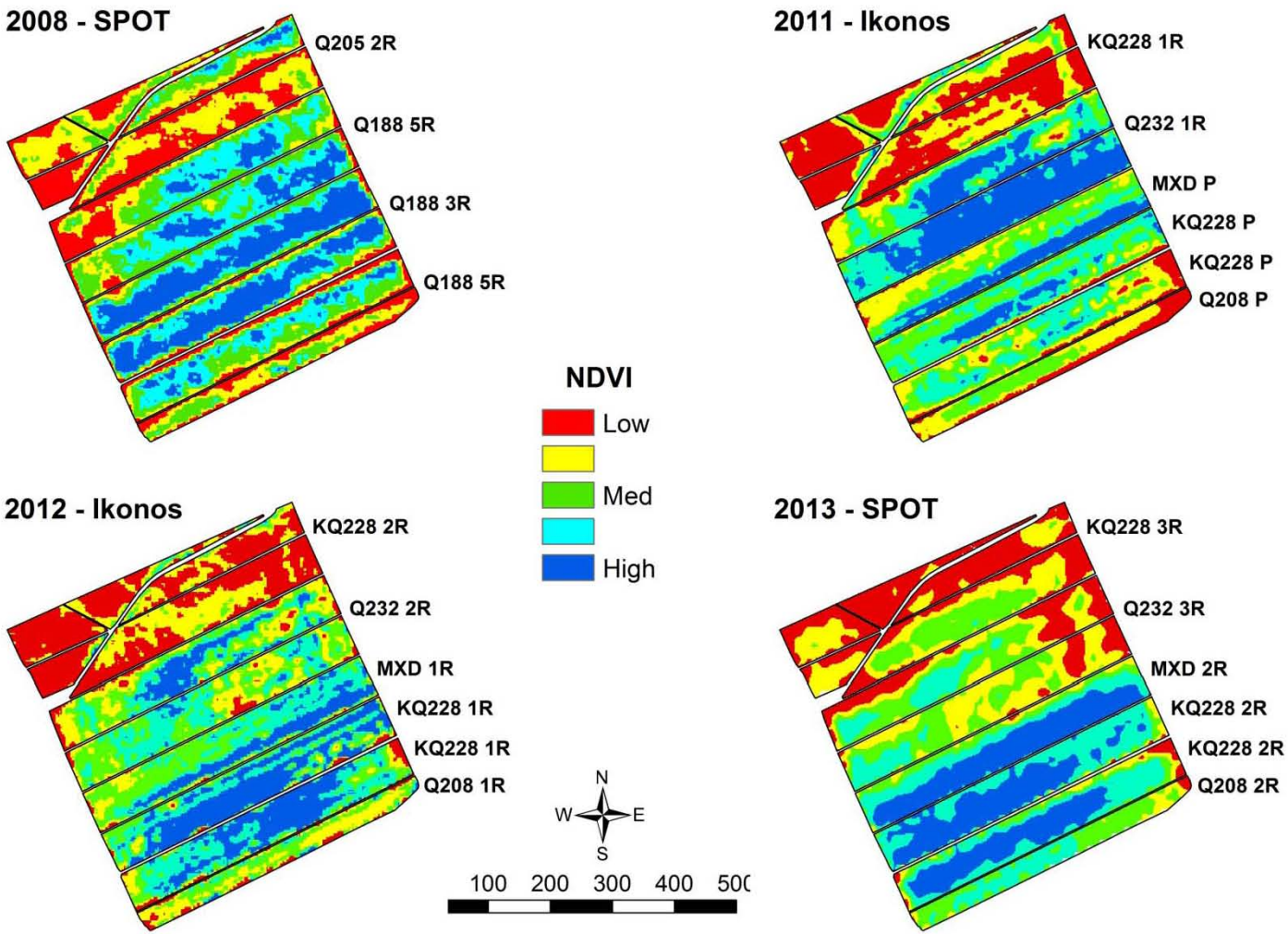

Figure 12.6 Satellite imagery collected for the Bundaberg study site over a six year period (2008-13). Also shown is the variety mix in the block; labels aligned with a sub-block boundary indicate that the listed variety is grown in both sub-blocks either side of the boundary.

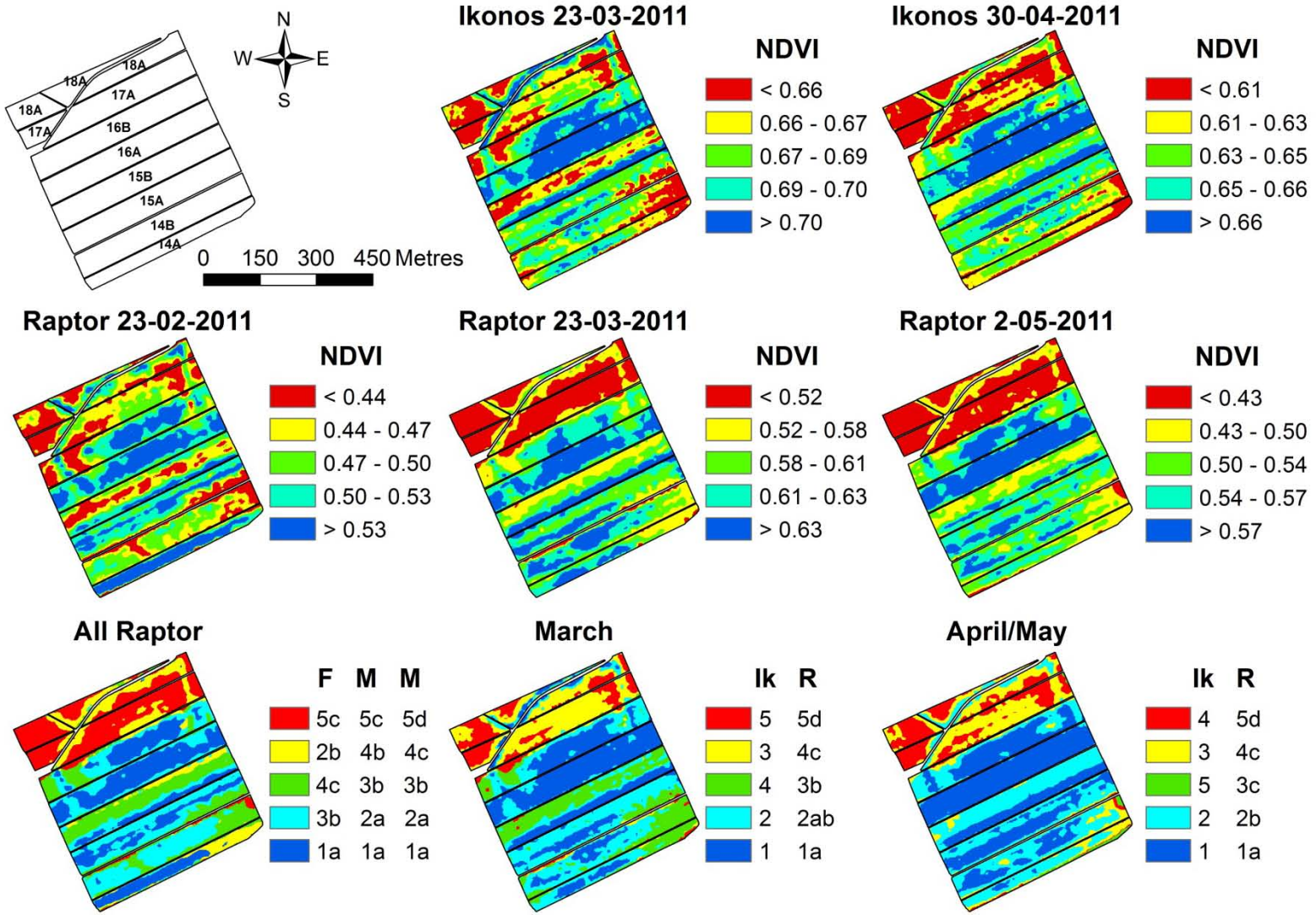

Figure 12.7 Imagery acquired during the 2011 season from either satellite (Ikonos) or airborne (Raptor) platforms in collaboration with SRDC Project DPI021 (Andrew Robson and David Lamb).

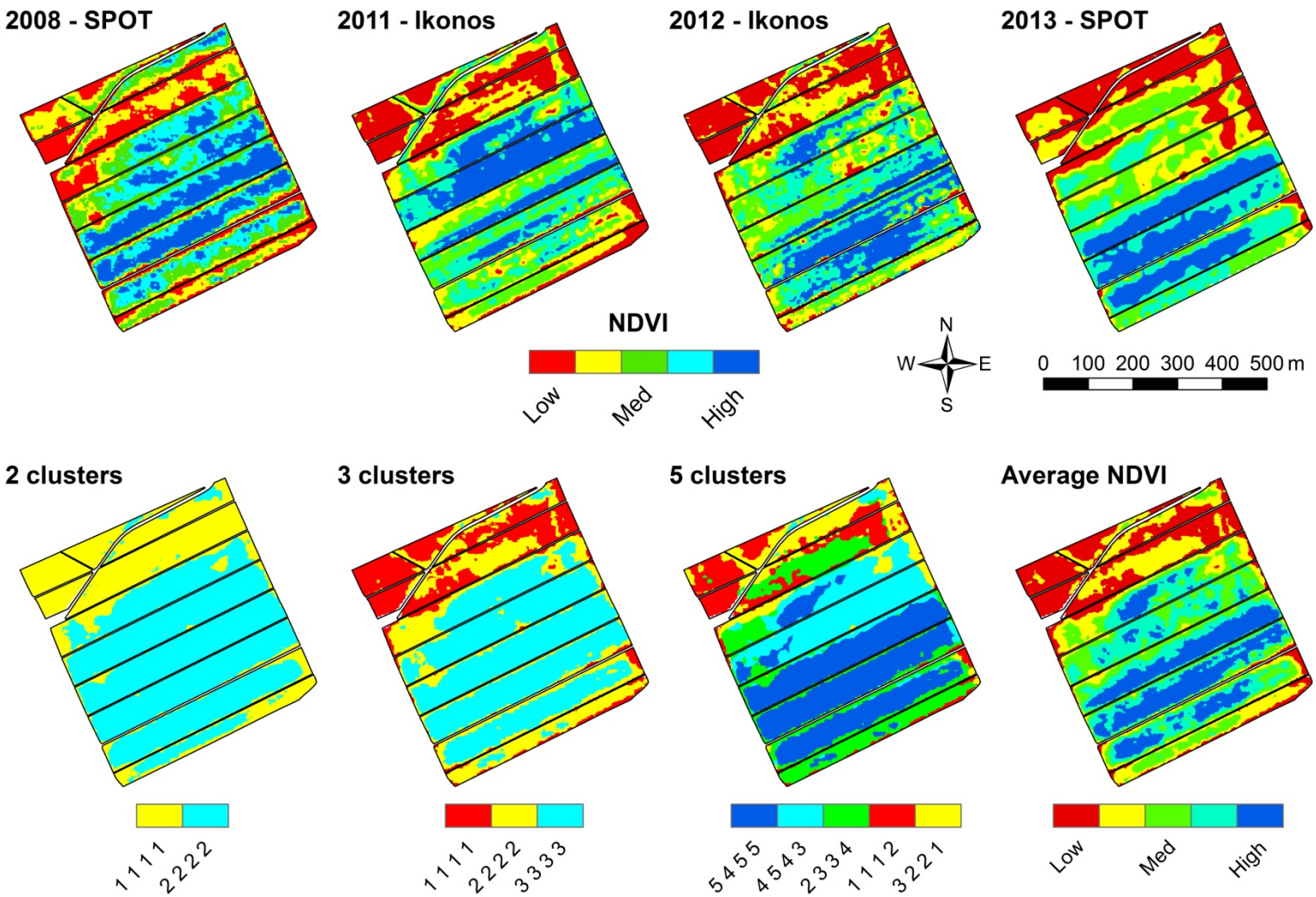

Figure 12.8 Cluster analysis (*k*-means) of satellite imagery acquired over a six year period. In the legends to the cluster maps, the numbers refer to the rank order of the clusters, where 1 is low (i.e. low NDVI) and 5 is high, in 2008, 2011, 2012 and 2013 respectively. The average image is derived from the average of normalised images (mean of zero, standard deviation of 1) for the 4 years.

as the same as that seen in the core imagery. Accordingly, an average image was also calculated. This was done by normalising the data within each component image (mean of zero, standard deviation of one) and averaging these normalised images. Normalised data were used for this analysis to remove the possibility of larger values in one year dominating lower values in another given that the imagery derives from passive sensing with the numbers consequently not having constant meaning from year to year. As can be seen in Figure 12.8, the average image can be seen to provide a robust representation of the pattern of variation in NDVI over time. Figure 12.8 also lends weight to the notion that variation in crop performance at this site is temporally stable.

Figure 12.9 shows the results of clustering the EM38 (Figure 12.2) and average image (Figure 12.8) data; solutions for 2-5 clusters are shown. The analysis clearly shows that based on this soil and imagery data, delineation of the study site into 2 or 3 potential management zones might be justified; both the rank order of NDVI and EM38 data and the significance of the difference between mean cluster EC_a values, evident in the 2-4 cluster solutions, breaks down when 5 clusters are used whilst the difference between the yellow cluster in the three zone solution and the yellow and green zones in the four cluster solution appears minor. Of course, the importance of the clusters depends to a large extent on variation in their yields.

Whilst the Hubert farm was the focus of much of the yield monitoring development work conducted in the project, events conspired against a complete coverage of yield data across the entire 24.7 study site; the replanting of blocks 14A and B and 15A and B in 2010 also presented a difficulty; Figure 12.6 indicates the variety mix and crop age. Thus, a limited area of yield data were available to complement the analysis done in Figure 12.9, as shown in Figure 12.10. It is apparent from Figures 12.3-12.10 that whereas there was temporal stability in the patterns of variation seen in remotely sensed imagery, variation in yield appeared much less stable.

In Figure 12.10, the yield data for sub-blocks 15A and B have been adjusted to an equivalent mean yield to that achieved in 16A and B (see Appendix 33 for an explanation of this process) to remove the possible effect of the different varieties in these sub-blocks having different yield potentials. In order to examine similarities in patterns of yield variation and possible association with other data layers, the yield maps for each year were further adjusted to an equivalent 2011 yield basis (mean of 87.6 t/ha; also explained in Appendix 33) before clustering.

Figure 12.11 shows the results of selected cluster analyses using the yield data; regrettably, this analysis was confined to sub-blocks 16A and B given that these were the only sub-blocks for which we had yield data in each year of the study. In Figure 12.11a, clustering of the adjusted yield data over four years suggests that whereas the mean cluster yields were significantly different ($p<0.05$) in both 2012 and 2013, there was no difference in 2010 and 2011. When the data were examined in year pairs (2010 and 2011 in Figure 12.11b; 2012 and 2013 in Figure 12.11c), the mean cluster yields were significantly different ($p<0.05$) in all cases. However, in both 2010 and 2011, the differences between the mean cluster yields would be unlikely to be considered sufficiently commercially significant to warrant consideration of some form of targeted management. Note that when the EC_a data were

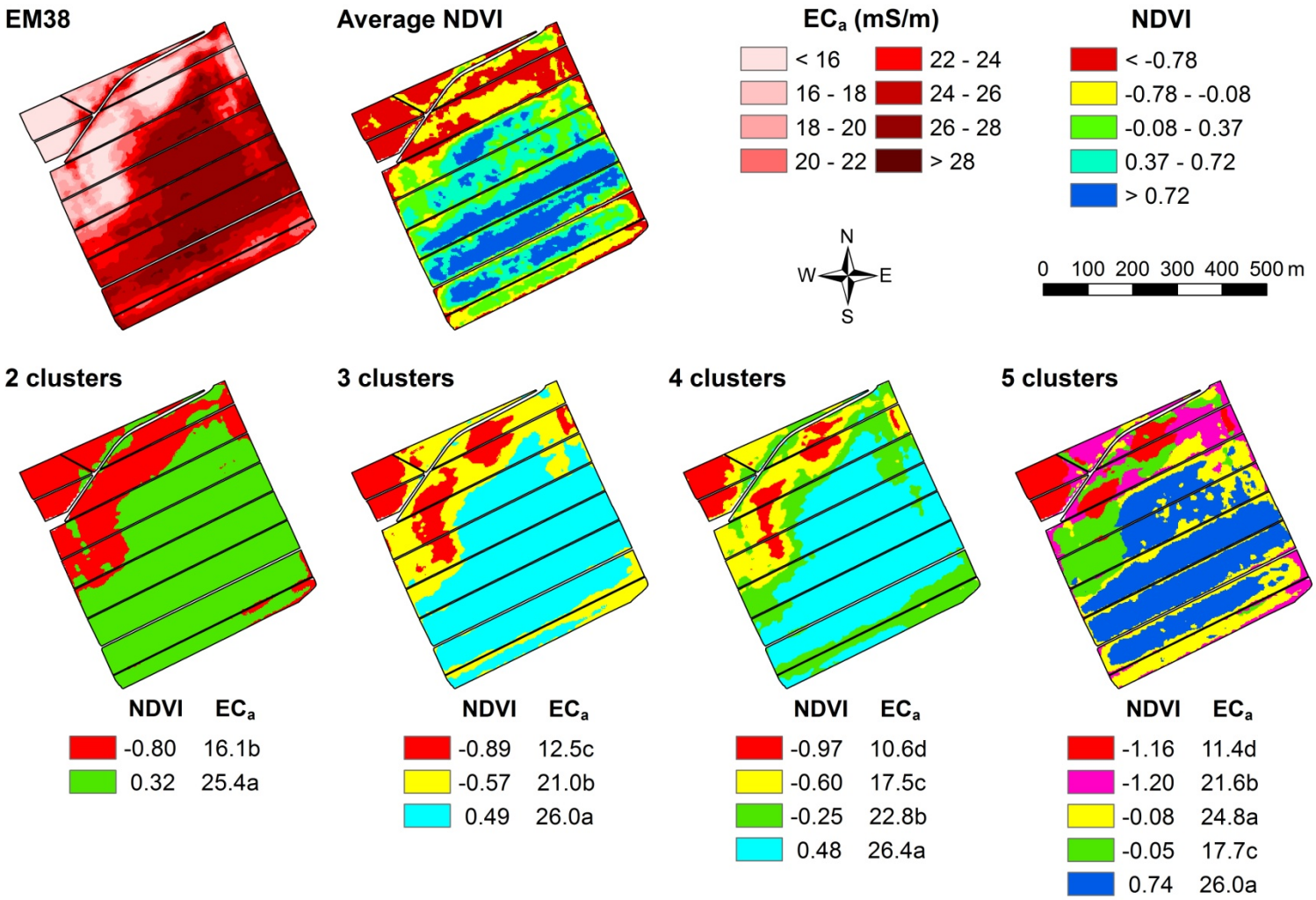

Figure 12.9 Cluster analysis (*k*-means) of EM38 soil conductivity data (ECa) and the average NDVI calculated over a six year period. In the cluster maps, the legend colours are matched to the colours in the average image to the extent possible, although as can be seen, this becomes problematic for the four and five cluster solutions. Mean cluster EC_a values followed by different letters are significantly different ($p<0.05$).

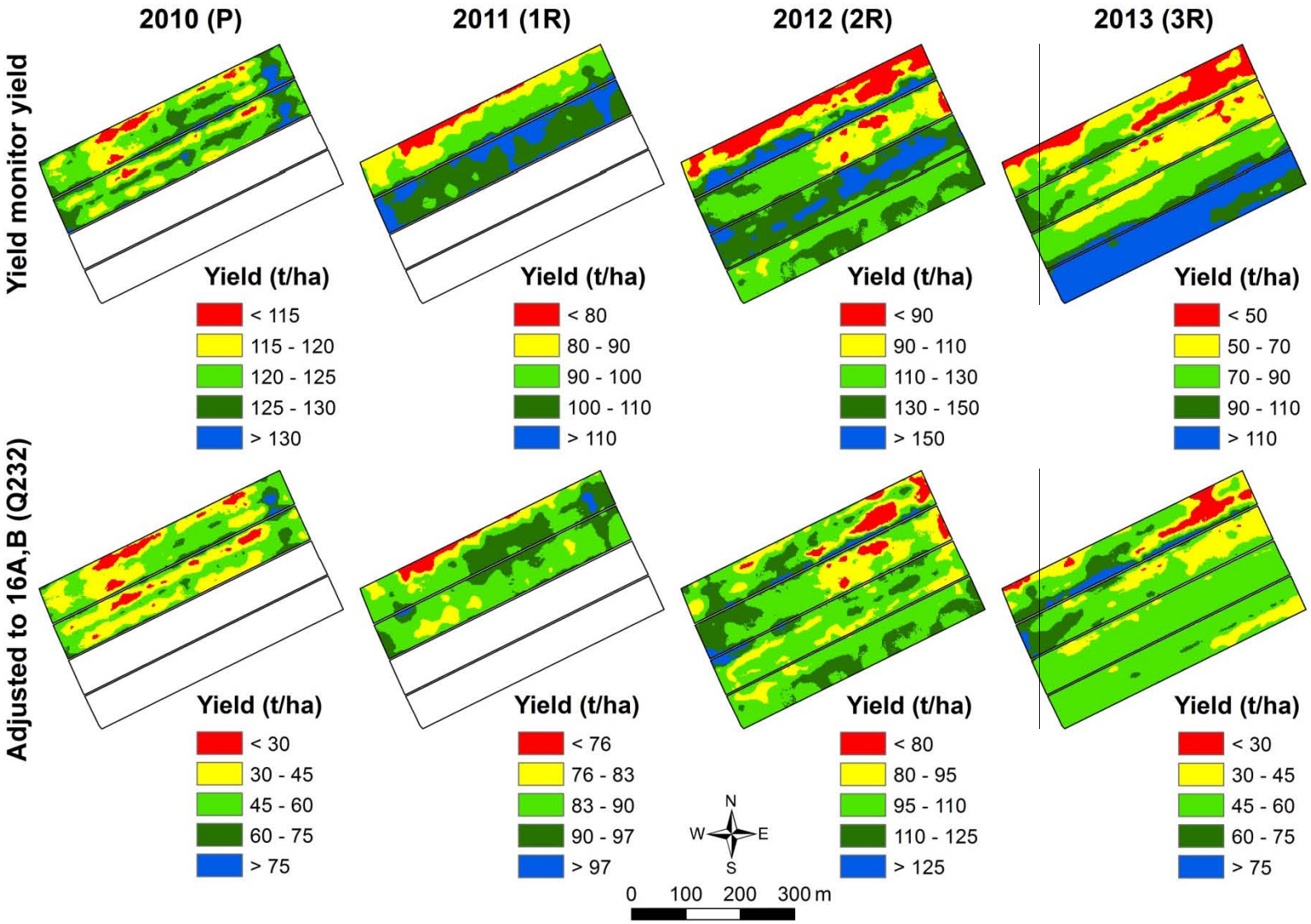

Figure 12.10 Yield maps obtained from the study site in the period 2011-13; note that these are confined to sub-blocks 15A and B and 16A and B.

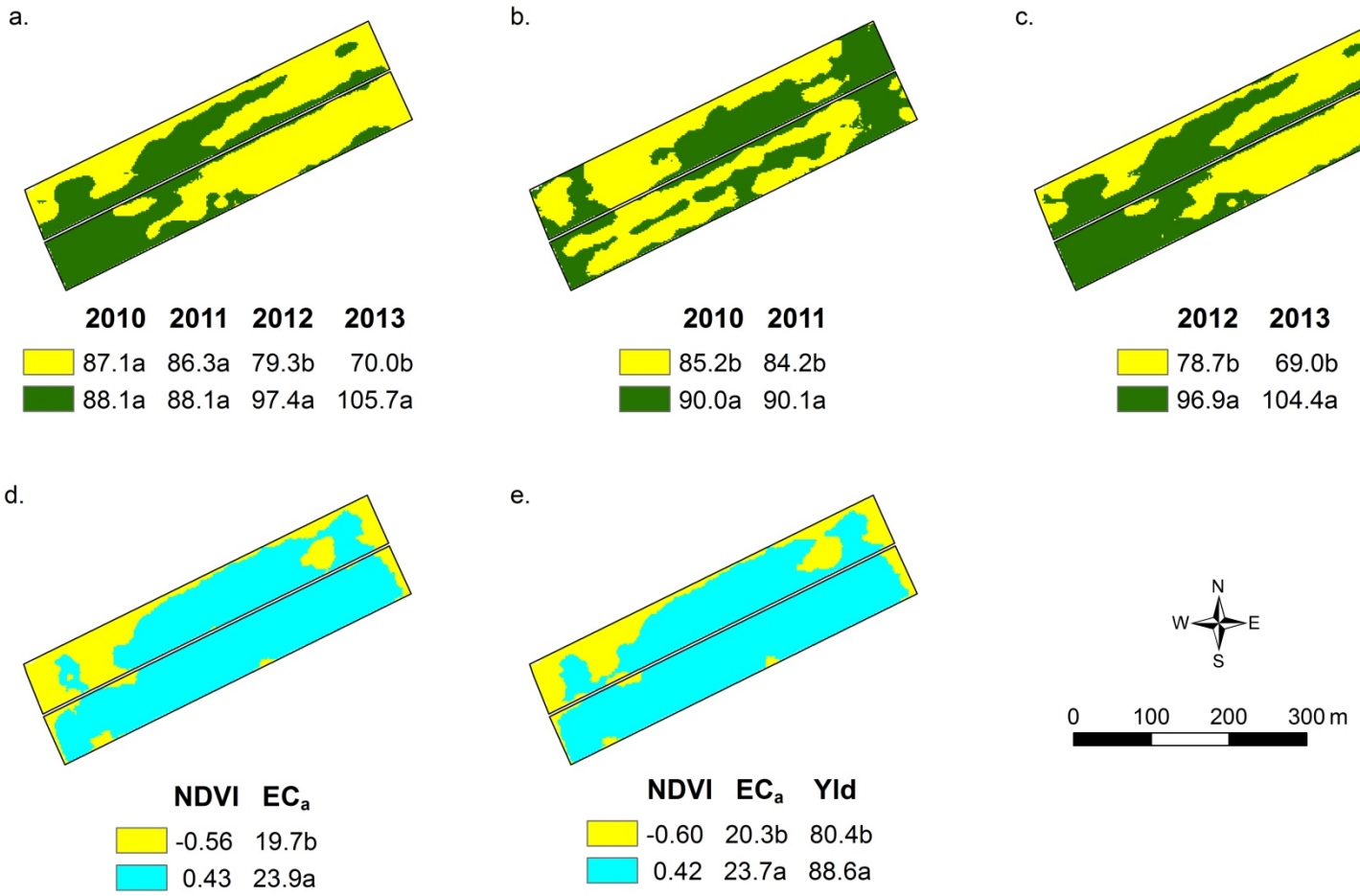

Figure 12.11 Selected cluster analysis for sub-blocks 16A and B. (a) yield data for the 2010-13 period; (b) for 2010-11; and (c) for 2012-13, in all cases (a-c) adjusted to a 2011 equivalent basis). (d) Average NDVI (Figure 12.8) and EM38 data (EC_a), and in (e) with average yield (2010-13, 2011 basis) also included. Cluster means followed by different letters in the same year or column are significantly different ($p<0.05$).

included in these analyses, the patterns of variation seen in Figures 12.11a-c remained essentially unchanged. However, and contrary to the analysis of imagery and ECa data, higher yields seemed to be associated with lower EC_a values. Given that the soils at this site are free draining, and that the variation in the EM38 survey is predominantly reflective of clay content, and therefore, presumably soil water holding capacity, this result seems counter intuitive and is likely an artefact. The striping evident in both Figures 12.10 and 12.11 suggests that in this instance, the yield monitor data may not be as reliable as hoped, perhaps due to the relatively narrow range of yield variation by comparison, for example, with our Burdekin study site (Appendix 13). The small area over which it was possible to do this analysis (6.7 ha) may also contribute to the uncertainty of the results. Note that when the average NDVI (2008-13; Figure 12.8) and ECa data for sub-blocks 16A and B are clustered (Figure 12.11d), the inferred interaction between soil properties and crop performance is as per the analysis for the whole study site (Figure 12.9). When the average yield (2010-13) is also included in the clustering, the expected relationship is retained, albeit with a difference between the cluster means yields of 8.2 t/ha (Figure 12.11e) – a difference that is approximately equivalent to 10% on the basis of the 2011 mean yield of 87.6 t/ha. Draping these data over the digital elevation model derived from the machinery guidance system used on the Hubert farm (Figure 12.12) suggests an uncertain topographic effect, again probably due to the small area and uncertainty over the yield data available.

It is to be hoped that further analysis can be undertaken over a wider area in the course of the new yield monitoring project (submitted as RB001). In the interim, the analyses reported here re-affirm the truism that remotely sensed imagery must be ground-truthed in order for it to be a robust basis for decision-making around targeted management.

Acknowledgments

We are indebted to Jay Hubert and the Hubert family for allowing us to conduct this work on their farm. Their assistance and support, along with that of their harvester crew has been greatly appreciated. We are also grateful to Dr Andrew Robson (University of New England; formerly QDAFF) for providing the remotely sensed imagery used in this study.

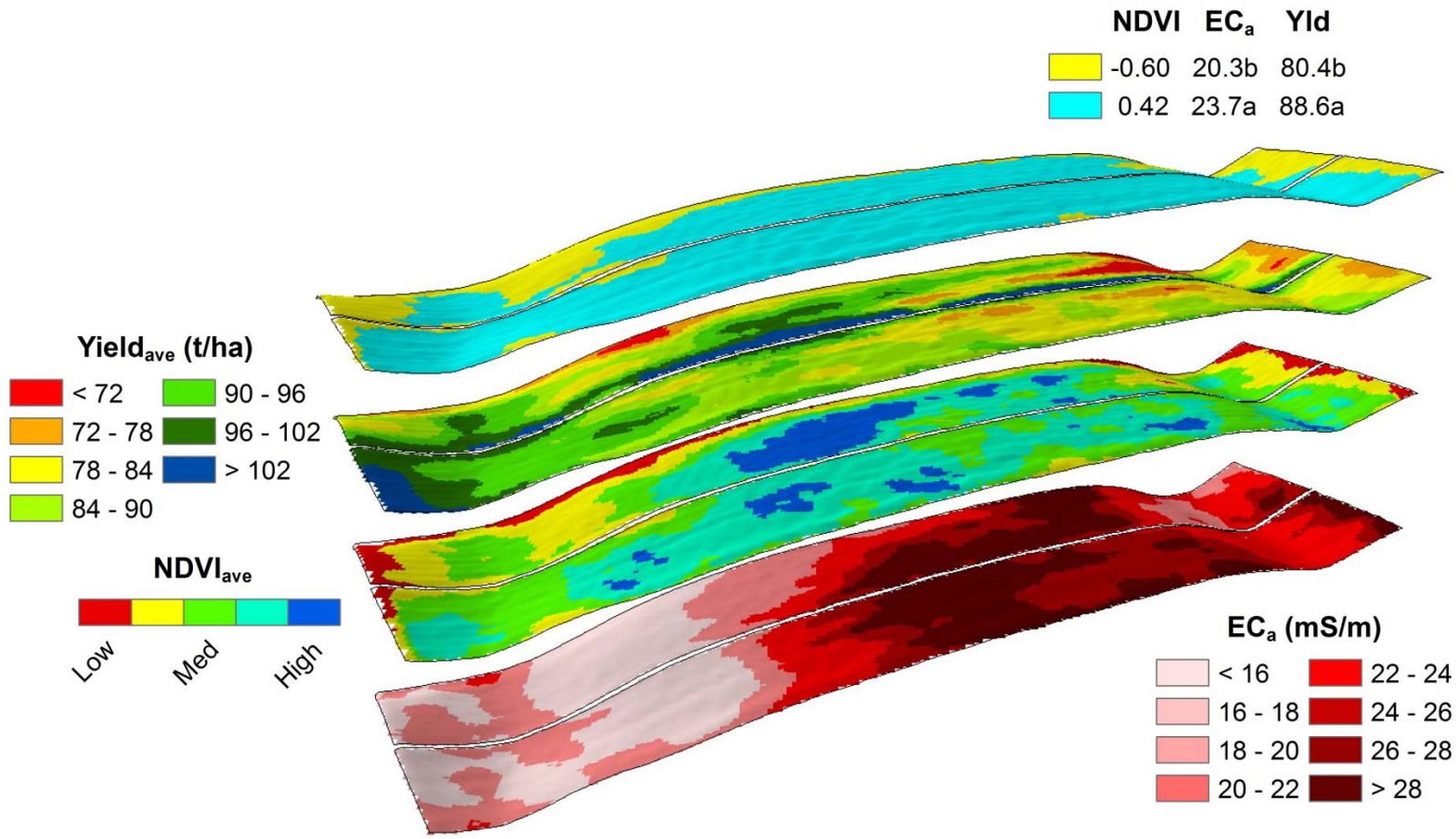

Figure 12.12 Alternative display of the data underpinning Figure 12.11e, draped over the digital elevation model of the site. Note that the range of elevation in sub-blocks 16A and B is 6.9 m. Here a vertical exaggeration of 7.5 times has been used.